Trans. Japan Soc. Aero. Space Sci.
Vol. 59, No. 2, pp. 56–63, 2016

Aerodynamic Characteristics of Low-Aspect-Ratio Wings with Various Aspect Ratios in Low Reynolds Number Flows*

Makoto MIZOGUCHI,[1)†] Yusuke KAJIKAWA,[2)] and Hajime ITOH[1)]

[1)]*Department of Aerospace Engineering, National Defense Academy, Yokosuka, Kanagawa 239–8686, Japan*
[2)]*Graduate School of Science and Engineering, National Defense Academy, Yokosuka, Kanagawa 239–8686, Japan*

The effect of the aspect ratio on the stall characteristics of low-aspect-ratio wings is experimentally investigated at a Reynolds number of 5.2×10^4. The aspect ratio ranges from 0.5 to 1.5 at intervals of 0.1. The aerodynamic coefficients of thin rectangular wings are measured in a low-speed wind tunnel. It is found that the aerodynamic characteristics of low-aspect-ratio wings are significantly sensitive to the aspect ratio. The maximum lift coefficient increases as the aspect ratio decreases toward unity. On the other hand, the difference in lift-to-drag ratio is negligible at large angles. Hysteresis during a stall occurs when the aspect ratio is within a narrow range. The span of the hysteresis loop has its peak at an aspect ratio of 1.0. The discussion also includes the analysis of lift components and flow visualization.

Key Words: Low-Aspect-Ratio Wing, Stall Hysteresis, Aerodynamic Characteristics, Low Reynolds Number Flows

1. Introduction

The understanding of wing characteristics at low Reynolds numbers is important for the development and control of low-speed, unmanned air vehicles. Hence, the aerodynamic characteristics of airfoils and high-aspect-ratio wings have been thoroughly studied at low Reynolds numbers.[1–7)] Moreover, the aerodynamics of low-aspect-ratio wings has also been investigated in low Reynolds number flows because some unmanned air vehicles use low-aspect-ratio wings.[4–10)] Aerodynamic hysteresis was frequently observed in the previous studies. Here, when the aerodynamic coefficients of a wing become multiple-valued with respect to the angle of attack, it is referred to as aerodynamic hysteresis. Aerodynamic hysteresis affects recovery from stall and spin conditions because it frequently occurs near the time of stalling. Hence, it is important to understand aerodynamic hysteresis during a stall.

Aerodynamic hysteresis is relatively common for thick wings at low Reynolds numbers. For example, the occurrence of aerodynamic hysteresis was reported by Schmitz[11)] for a thick wing with an aspect ratio of 5.0. Moreover, various studies on aerodynamic hysteresis have been conducted for two-dimensional airfoils and high-aspect-ratio wings.[1–3,12–16)] Aerodynamic hysteresis of airfoils can be classified into two types: clockwise hysteresis and counterclockwise hysteresis.[2,3)] Regarding clockwise hysteresis, it is known that the bursting of a laminar separation bubble causes the hysteresis. Counterclockwise hysteresis occurs when a long bubble transforms into a short bubble as the angle of attack increases. It was shown that the Reynolds number,[1–3,12)] turbulence intensity[1,2,13–15)] and acoustic disturbance[13,14,16)] affect the hysteresis of airfoils and high-aspect-ratio wings. For example, Hoffmann[15)] studied the influence of turbulence intensity on a wing with an aspect ratio of 2.9. The elimination of hysteresis was shown in a flow with large turbulence intensity. This is considered to be caused by the enhanced transition of the separated boundary layer. Marchman et al.[13)] also showed that hysteresis is sensitive to turbulence intensity and acoustic disturbance. For the Reynolds number, Mueller[2)] reported the elimination of hysteresis by increasing the Reynolds number for the Lissaman 7769 and Miley M06-12-128 airfoils. This is also due to the behavior of the laminar separation bubble on airfoils. Thus, for airfoils and high-aspect-ratio wings, it is thought that aerodynamic hysteresis is caused by the influence of low Reynolds numbers. However, the mechanism of hysteresis is not fully understood, even for wings with moderate-to-large aspect ratios. Moreover, little attention has been given to wings with low-aspect-ratios.

Regarding low-aspect-ratio wings, Winter[17)] studied the aerodynamics at Reynolds numbers ranging from 3.0×10^5 to 1.7×10^6 in the 1930s. Hysteresis during a stall was observed for an aspect ratio of 1.0 in his study. However, little attention has been given to the stall hysteresis of low-aspect-ratio wings. Ananda et al.[18)] recently showed that stall hysteresis does not occur for thin, low-to-moderate aspect ratio wings at low Reynolds numbers. The aspect ratios were between 2.0 and 5.0 in their study. Torres and Mueller[8)] also stated that no hysteresis was observed in their experiments (the aspect ratios in their study ranging from 0.5 to 2.0). They presumed that the small thickness resulted in the elimination of hysteresis. The present authors also conducted experimental studies on the aerodynamic characteristics of low-aspect-ratio wings at low Reynolds numbers.[7,9,19)] The occurrence of stall hysteresis was observed for wings with an aspect ratio of 1.0, although the data for aspect ratios of 1.5 and 0.5 did

*Partly presented at the 51st Aircraft Symposium, Nov. 20–22, 2013. Received 2 April 2015; final revision received 18 September 2015; accepted for publication 19 October 2015.
†Corresponding author, makoto@nda.ac.jp

not show any hysteresis. Okamoto and Azuma[6] and Shields and Mohseni[10] also reported similar results. Thus, several previous studies reported the occurrence of hysteresis only for wings with an aspect ratio of 1.0. Therefore, it seems that the occurrence of stall hysteresis depends on the aspect ratio. Marchman et al.[20,21] stated, for relatively thick wings, that hysteresis during a stall becomes more pronounced as the aspect ratio increases. Here, the aspect ratios adopted in their study were 4.0 and 2.0. They presumed that stall hysteresis would be eliminated when the aspect ratio decreases toward 1.0. This is contradictory to some of the previous results stated above. From the comparison, it seems that the mechanism of stall hysteresis for low-aspect-ratio wings is different from that for high-aspect-ratio wings. Thus, the effect of the aspect ratio on the stall characteristics of low-aspect-ratio wings still remains unclear. Moreover, aerodynamic data for various aspect ratios will also benefit further development of unmanned vehicles with low-aspect-ratio wings.

In the present study, the effect of the aspect ratio on the occurrence of aerodynamic hysteresis is investigated in low Reynolds number flows. The aerodynamic coefficients of thin rectangular wings are evaluated using various aspect ratios. The discussion includes the analysis of aerodynamic performance, lift factors and flow visualization.

2. Experimental Setup

A flat-plate airfoil was used for the present study. The leading- and trailing-edges are flat, so that the chordwise cross-section of the model is rectangular. Each wing model has a rectangular planform and flat side edges. The chord length and thickness of each model are 90 mm and 1 mm, respectively. The aspect ratio varies from 0.5 to 1.5 in increments of 0.1. The models are made of dark, polyvinyl-chloride plate.

The aerodynamic coefficients of the wings were evaluated in a low-speed wind tunnel at the National Defense Academy of Japan. A schematic of the tunnel is shown in Fig. 1. The test section is an open-type. The models were installed 90 mm downstream from the nozzle exit, which has a diameter of 400 mm. The turbulence intensity was about 1.4%. The Reynolds number based on the chord length was 5.2×10^4. The aerodynamic coefficients were measured using a three-component balance. The inverted models were supported by the strut of the balance, as shown in Fig. 2. The strut was connected to the model 1/4 chord downstream from the leading-edge along the centerline of the wing. The angle of attack was adjusted between -10 deg and 50 deg. The sweep of the angle started at -10 deg and the angle increased at increments of 1 deg. After completing the sweep of increasing angles of attack, each model was brought back to the initial angle at the same angle intervals. The tare and strut influence were evaluated separately. The aerodynamic coefficients were corrected using the boundary correction method.[22] Output data from the balance system was acquired at a sampling frequency of 100 Hz, with 500 individual data points for each output.

The oil flow method was used for flow visualization on the wing surface. A mixture of titanium dioxide, liquid paraffin and oleic acid was applied to the suction side of the model surface. The model was exposed to the main flow after adjusting the angle of attack. Observations were made until a steady flow pattern was obtained. Still and moving images were recorded using a digital camera. The moving images were used to aid in the interpretation of the flow structures.

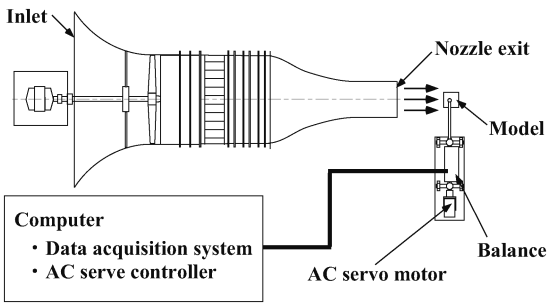

Fig. 1. Low-speed wind tunnel.

3. Results and Discussion

3.1. Uncertainty analysis

The uncertainty in the measurements was analyzed using the approach of Coleman and Steele.[23] The uncertainty depends on the bias and precision limits. Here, the precision limit indicates the repeatability of the measurements, and the bias limit results from the estimated systematic uncertainties in each component used in the measurements. The systematic uncertainty in the force measurements (approximately 10 mN) was dominant for the bias limit in the present study. The precision limit was comparable to the bias limit. When the aspect ratio AR decreases, the aerodynamic force decreases due to the reduction in wing area. The resulting uncertainties in the lift coefficient C_L and drag coefficient C_D were estimated to be ± 0.03 for $AR = 1.5$ and ± 0.05 for $AR = 0.5$. The representative results of the uncertainty analysis are shown in Figs. 3 and 4 for $AR = 1.0$ and 0.5. The error bars represent a 95% confidence interval. It is thought that these uncertainties are acceptable for the discussion in the present study. To validate the measurement system, Figs. 3 and 4 include redigitalized data obtained by Okamoto and Azuma[6] at Reynolds numbers around 1.5×10^4. Their model shape is comparable to that in the present study. The present results agree well with the existing data within the uncertainty bounds, except under near-stall conditions. It is believed that the discrepancies near stalling are caused

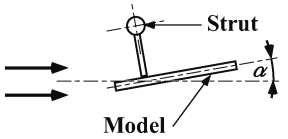

Fig. 2. Mounting of test model.

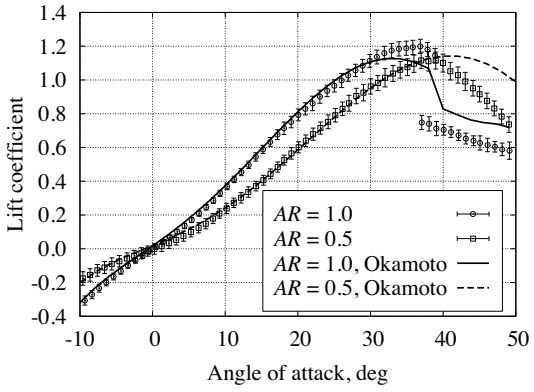

Fig. 3. Uncertainty in C_L for $AR = 1.0$ and 0.5.

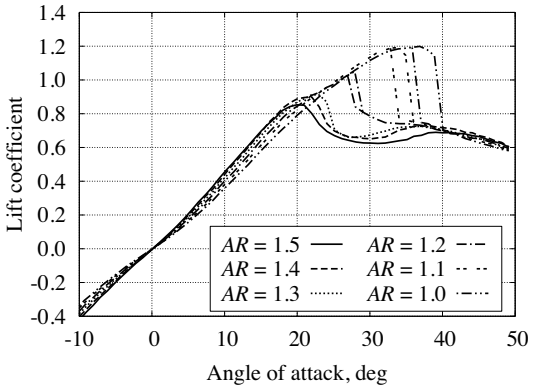

Fig. 5. C_L vs AR for $AR = 1.5$ to 1.0.

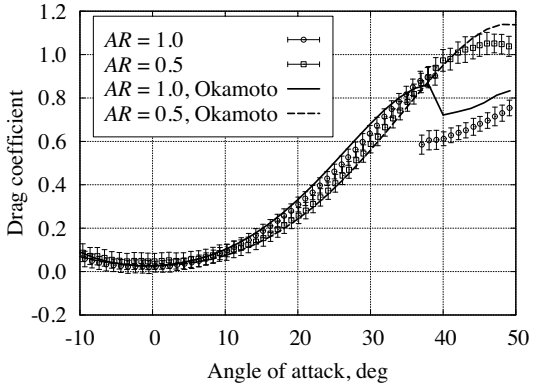

Fig. 4. Uncertainty in C_D for $AR = 1.0$ and 0.5.

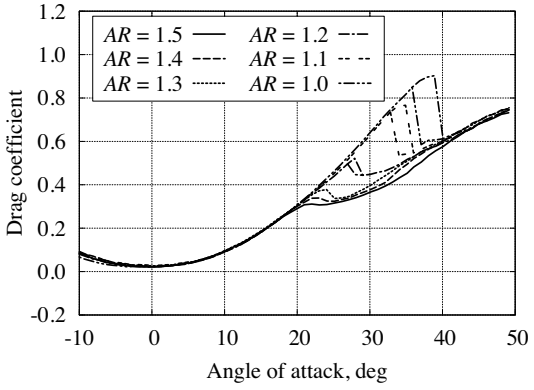

Fig. 6. C_D vs AR for $AR = 1.5$ to 1.0.

by experimental setup variations between these studies and the differences in the Reynolds number and thickness ratio. The pitching moment coefficient was also measured in experiments. However, the uncertainty in the pitching moment coefficient was relatively large; the percentage uncertainty in the pitching moment coefficient was about 20%. It is considered that discussing the pitching moment coefficient is difficult because of such large uncertainty. Hence, we limit our discussion to the effect of the aspect ratio on C_L, C_D and related factors in the present study.

3.2. Aerodynamic coefficients

Figures 5 to 8 show the aerodynamic coefficients of the models with various aspect ratios. The differences in C_L and C_D are very small when the aspect ratio ranges from 1.5 to 1.3, as shown in Figs. 5 and 6. The maximum lift coefficient was obtained at around 20 deg in these cases. Here, $\alpha_{\max}$ is defined as the angle at which C_L reaches the maximum value. Figure 5 shows that $\alpha_{\max}$ increases slightly as the aspect ratio decreases. The values of C_L when increasing the angle of attack correspond to those for decreasing the attack angle. Thus, aerodynamic hysteresis does not occur when the aspect ratio is between 1.5 and 1.3.

When the aspect ratio decreases to 1.2 or lower, the aerodynamic characteristics change considerably, as shown in Figs. 5 and 6. The present study shows that a slight variation in aspect ratio leads to a significant change in aerodynamic characteristics. The value of $\alpha_{\max}$ increases up to 28 deg for $AR = 1.2$ and increases further as the aspect ratio decreases toward 1.0. The maximum lift coefficient also increases significantly when the aspect ratio decreases toward unity. This tendency quantitatively agrees with that at $Re = \mathrm{O}(10^6)$.[24] Torres and Mueller[8] also found a similar increase in the maximum C_L for thin rectangular wings at a Reynolds number of 1.0×10^5. Moreover, their data for $AR = 1.25$ is comparable to the present results ($AR = 1.5$ to 1.3 at $Re = 5.2 \times 10^4$) shown in Fig. 5. These comparisons indicate that the influence of the Reynolds number is small.

When the aspect ratio is 1.0 or lower, the variation in aerodynamic characteristics due to the aspect ratio becomes small, relative to that for $AR = 1.3$ to 1.1. The lift coefficient shows a gradual decrease after C_L reaches the maximum value. The drag coefficient also increases gradually, although the rate of increase for C_D decreases at around $\alpha_{\max}$. These tendencies are qualitatively similar among aspect ratios between 1.0 and 0.5. For $AR = 0.6$, although scatter exists among the experimental results, peculiar increases in lift and drag were observed in the post-stall region of the experiments (the values are not shown in Figs. 7 and 8). Similar increases in C_L were also reported by Winter[17] and Torres and Mueller.[8] It is believed that the small vibration of wing models is a probable factor for such peculiar increase.

It is found that the aerodynamic coefficients become multiple-valued with respect to the attack angle when the aspect

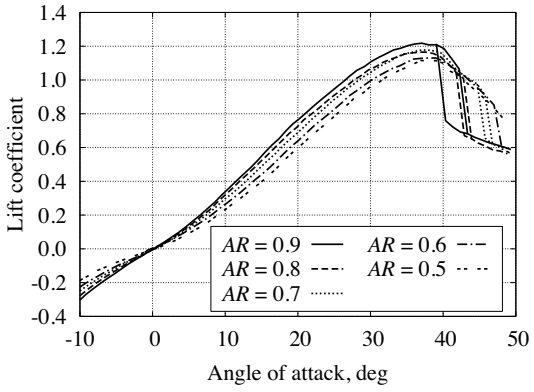

Fig. 7. C_L vs AR for $AR = 0.9$ to 0.5.

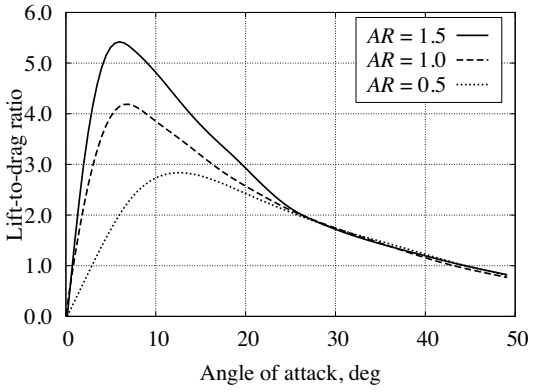

Fig. 9. Lift-to-drag ratio.

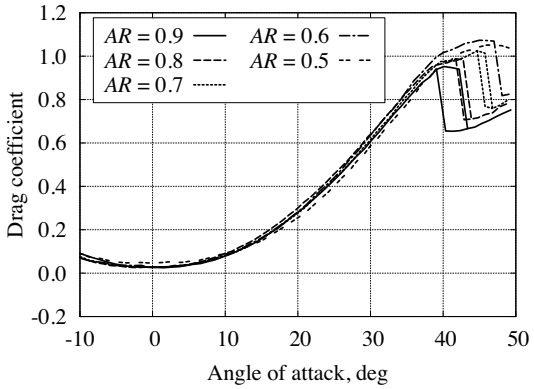

Fig. 8. C_D vs AR for $AR = 0.9$ to 0.5.

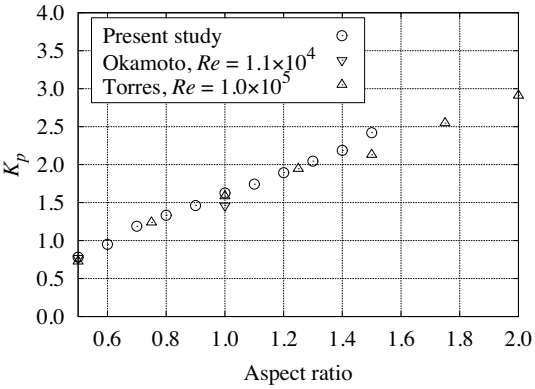

Fig. 10. Potential lift factor as a function of AR.

ratio is between 1.2 and 0.7. The hysteresis shown in Figs. 5 to 8 can be classified as clockwise hysteresis.[1–3] The stall hysteresis ends with abrupt changes in C_L and C_D. The hysteresis loop shifts to the right as the aspect ratio decreases. Furthermore, it is found that stall hysteresis disappears when the aspect ratio decreases to 0.6 or lower. Rapid reductions in C_L and C_D can be seen for $AR = 0.6$ at 48 deg while such abrupt change is not shown for $AR = 0.5$. For the aerodynamic characteristics of the model with an aspect ratio of 0.5, additional experiments were conducted for the angle of attack above 50 deg, although the result is not shown here. It was found that the aerodynamic coefficients for $AR = 0.5$ also decrease abruptly without stall hysteresis. These observations indicate that sudden reductions in aerodynamic coefficients are not always accompanied by hysteresis during a stall. The differences in C_L and C_D disappear after stalling. This indicates that the flow is totally separated regardless of the aspect ratio after the hysteresis during a stall terminates. The stall hysteresis will be further discussed in Section 3.4.

3.3. Lift-to-drag ratio

The lift-to-drag ratio as a function of the attack angle is shown in Fig. 9. When the angle of attack is at around 25 deg or lower, the lift-to-drag ratio decreases as the aspect ratio decreases. This is because C_L depends on the aspect ratio while the difference in C_D is negligible. The maximum lift-to-drag ratio decreases as a function of the aspect ratio. Moreover, the angle at the maximum lift-to-drag ratio increases as the aspect ratio decreases. However, the difference due to the aspect ratio disappears when the angle of attack is around 30 deg or higher. We analyzed the lift components using Lamar's method.[25] The lift coefficient can be divided into a potential lift component C_{L_p} and a vortical lift component $C_{L_{vor}}$ as described by the following equation.

$$C_L = C_{L_p} + C_{L_{vor}} \tag{1}$$

Here, C_{L_p} and $C_{L_{vor}}$ are expressed by $K_p \sin\alpha \cos^2\alpha$ and $K_v \cos\alpha \sin^2\alpha$, respectively. Lift factors K_p and K_v indicate each lift component. In the present study, a least-square multiple regression analysis was used to determine these parameters.[7,9] The analyzed results of the lift factors are shown in Figs. 10 and 11. Figures 10 and 11 include the data obtained by other researchers.[6,8] The reference data was obtained at Reynolds numbers of 1.1×10^4 and 1.0×10^5. The results of the present study quantitatively agree with the reference data. The comparison indicates that the lift slope K_p is not sensitive to the Reynolds number when the aspect ratio is low. Moreover, as is well known, the potential lift component decreases as the aspect ratio decreases. Figure 11 indicates that the vortical component increases when the aspect ratio decreases; the effect of the Reynolds number is thought to be small. The vortical lift components at 5 deg are rated to be 5% of the total lift for $AR = 1.5$, 13% for $AR = 1.0$ and 25% for $AR = 0.5$. Thus, the potential lift is more dominant

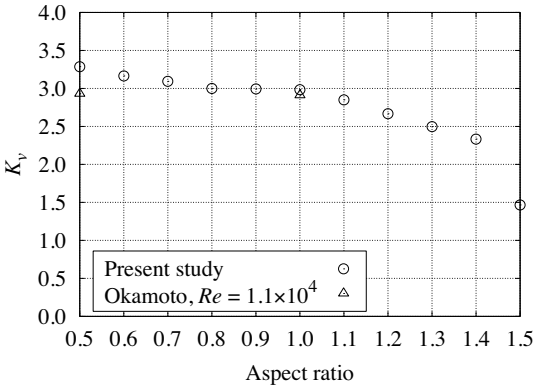

Fig. 11. Vortical lift factor as a function of AR.

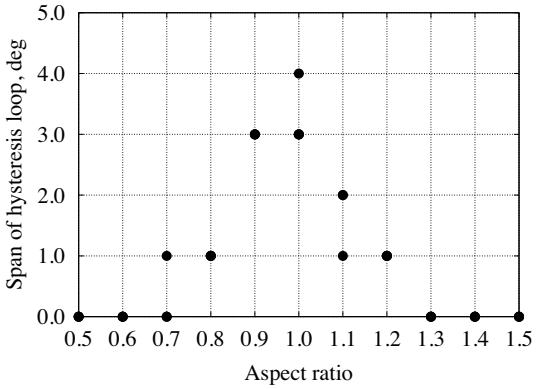

Fig. 12. Span of hysteresis.

at low angles. The difference in lift-to-drag ratio is mainly caused by the potential lift.

3.4. Stall hysteresis of low-aspect-ratio wings

Stall hysteresis was observed when the aspect ratio was between 0.7 and 1.2, as stated previously. In the present study, the span of the hysteresis loop is introduced to understand the stall characteristics of low-aspect-ratio wings. The span of the hysteresis loop is defined by the angle-of-attack range where the aerodynamic coefficients become multiple-valued in terms of the attack angle. For example, the values of C_L for increasing the angle of attack differ from those for decreasing the angle between 40 deg and 42 deg for $AR = 0.9$, as shown in Fig. 7. Hence, the span of the hysteresis loop is determined to be 3 deg in this case. The experimental data shows some scatter in the span of the hysteresis loop. Hence, the individual results are plotted in Fig. 12. Figure 12 shows that the occurrence and span of hysteresis clearly depend on the aspect ratio. The span of the hysteresis loop has its peak at an aspect ratio of 1.0. Thus, low-aspect-ratio wings are closely related to hysteresis during a stall when the aspect ratio is around 1.0. Marchman et al.[21] presumed that hysteresis during a stall tends to disappear as the aspect ratio decreases toward unity. However, the present study finds that there is a narrow region of the aspect ratio in which stall hysteresis occurs. This is the reason why several studies[6,7,9,10,19] reported the occurrence of stall hysteresis only for an aspect ratio of 1.0, as stated previously. Moreover, Torres and Mueller[8] stated that hysteresis was not observed for an aspect ratio of 1.0 in their study. Therefore, it is thought that the occurrence of stall hysteresis depends not only on the aspect ratio, but also on other factors. The effect of other parameters on the hysteresis of low-aspect-ratio wings was recently reported by the present authors (the results can be found in Mizoguchi et al.[26]). In summary, it was found that the thickness ratio of wings affects the size of the hysteresis loop. The span of the hysteresis loop also depends on the Reynolds number and turbulence level of the flows.[26] Here, the Reynolds number, turbulence intensity and geometry of the model adopted by Torres and Mueller[8] are almost the same as those used by Shields and Mohseni.[10] The aspect ratio is 1.0 in each study. However, Shields and Mohseni observed stall hysteresis, whereas Torres and Mueller stated that no hysteresis was observed. The cause of this discrepancy still remains unclear, and further studies are needed.

Hysteresis during a stall was observed for low-aspect-ratio wings in the present study. For low-aspect-ratio wings, the occurrence of stall hysteresis was reported even at relatively high Reynolds numbers.[17] Moreover, in low Reynolds number flows, it was found that the hysteresis loop of low-aspect-ratio wings becomes larger as the Reynolds number increases.[26] Therefore, the occurrence of stall hysteresis is not limited to low Reynolds numbers when the aspect ratio is low.

3.5. Flow visualization

Figure 13 shows the results of flow visualization using the oil flow method. The aspect ratio was kept constant at a value of 1.0 in Fig. 13. The oil moves along the flow when the flow is attached to the surface. In the attached flow region, little oil mixture remains and the dark model surface can be seen. On the other hand, the light oil film remains or moves upstream in reverse flows. Here, the oil film also flows down due to gravity, particularly at large angles. Hence, it should be noted that the oil film patterns at large angles result from the balance between the upstream motion in the reverse flow and the downstream flow due to gravity. Therefore, the flow reattachment can be observed qualitatively as the line pattern of the oil film. Figure 13 includes a schematic of the reattachment line and the direction of oil motion.

The white region near the leading-edge shown in Fig. 13(a) denotes a leading-edge separation bubble. The downstream end of the white region indicates the approximate reattachment line. The size of the separation bubble decreases around the wingtip. When the angle of attack increases, the separation bubble grows, as shown in Fig. 13(b). The reattachment line becomes obscure around the center of the wing at 10 deg. The separated flow fails to reattach along the centerline at 15 deg, as shown in Fig. 13(c). When the angle of attack is less than or equal to 15 deg, the flow structures are qualitatively similar with those for an aspect ratio of 1.5, although the result is not shown here.

Figure 13(d) shows the visualized result at 25 deg. A convex line can be seen around the center of the wing. There is a

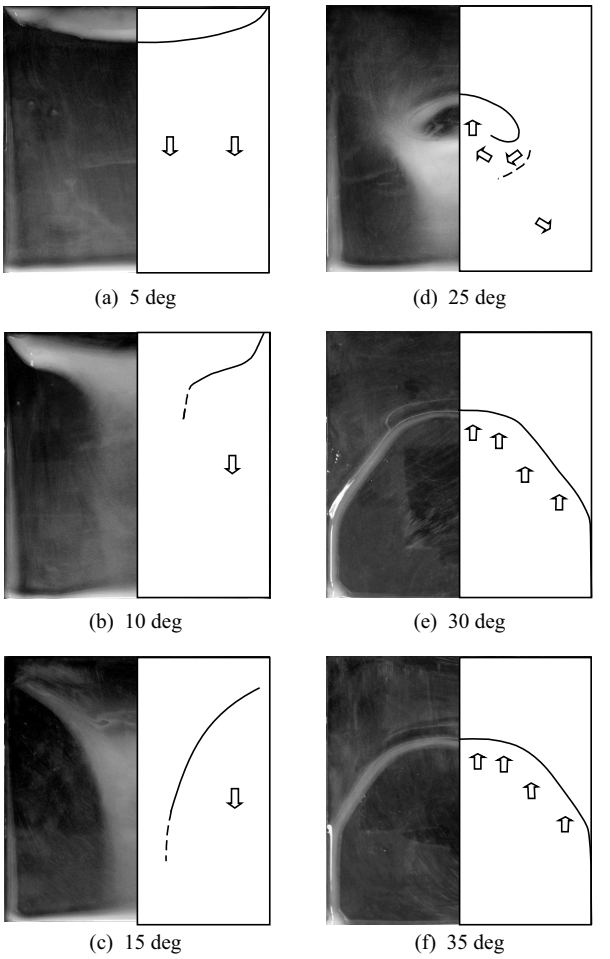

Fig. 13. Surface flow visualization for $AR = 1.0$.

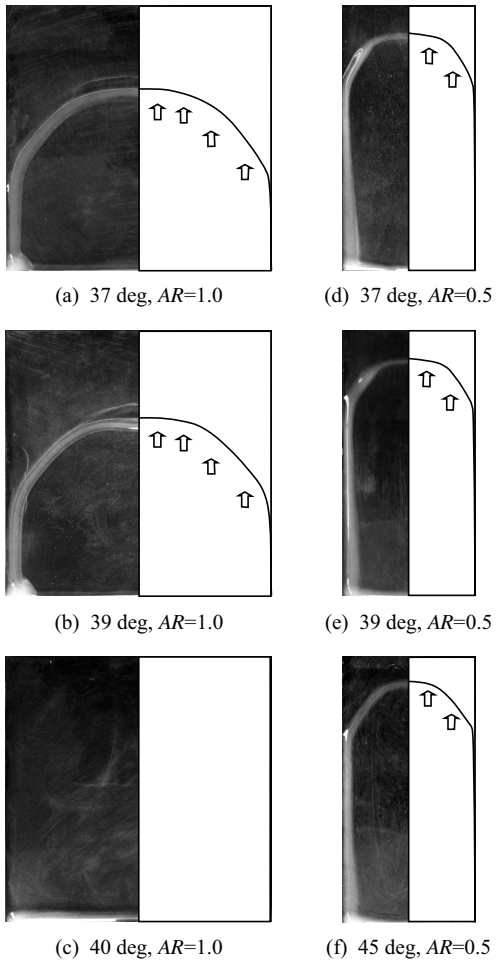

Fig. 14. Surface flow visualization near stalling.

white region downstream of the convex line. The line ends with a pair of counter-rotating swirling flows. These swirl structures were observed for $AR = 1.0$ when the angle of attack was between 20 deg and 27 deg in the present study. Thus, it is found that a change in the flow structure occurs at such moderate angles. Winkelmann and Barlow[27] found a mushroom-shaped pattern with two counter-rotating nodes after stalling using a rectangular wing with $AR = 3.5$. The flow pattern is quite similar to that shown in Fig. 13(d). Yon and Katz[28] also reported two circulating nodes (referred to as stall cells) over a narrow range of the attack angle beyond the stalling point. When the stall cells existed, the mean pressure was essentially constant but large-amplitude pressure fluctuations occurred in their study. Kajikawa et al.[19] visualized chordwise flows on a wing surface for $AR = 1.0$. It was shown that the separated shear layer forms a leading-edge separation bubble at 10 deg: the shear layer rolls up to form vortices, which are unsteadily shed from the edge of the shear layer at 20 deg.[19] These chordwise flows are consistent with the results of flow visualization in the present study. It is believed that the shedding vortices are related to pressure fluctuation, such as that observed by Yon and Katz.[28] In the present study, stall cells were not clearly observed for an aspect ratio of 1.5 at $\alpha = 20$ deg, although weakly swirling nodes could be seen in the corresponding moving images. However, the stall cells were observed at $\alpha = 20$ deg when the aspect ratio was reduced to 1.2. Moreover, the oil film for $AR = 1.2$ uniformly flows downstream at 30 deg. It is thought that the flow structure changes from the stall cells to a wake-like pattern after stalling. Yon and Katz[28] also stated that the surface pattern abruptly changed when the angle of attack increased beyond stalling; the change was accompanied by a sudden loss of lift. Thus, when the aspect ratio is 1.2 or higher, increasing the attack angle further beyond stalling causes the breakdown of the stall cells and an abrupt reduction in lift, as shown in Fig. 5.

When the aspect ratio is 1.0, the flows still remain reattached for $\alpha = 30$ deg and 35 deg, as shown in Figs. 13(e) and 13(f). Convex lines can be seen in Figs. 13(e) and 13(f). The flow patterns completely differ from those at 25 deg or lower. Such convex lines could not be seen for $AR = 1.2$. However, similar patterns were observed for smaller aspect ratios. Okamoto and Azuma[6] also reported similar results of flow visualization for $AR = 1.0$. Thus, it is found that the flow structure changes from the stall cells to the flows such as those shown in Figs. 13(e) and 13(f) if the aspect ratio is sufficiently small. The change in the flow structure is thought to cause the increase in stall angle and the maximum lift coefficient, as shown in Section 3.2.

Figure 14 shows the oil film patterns in the hysteresis loop

for $AR = 1.0$. The flow structure remains quite similar when the angle of attack is between 30 deg and 39 deg, as shown in Figs. 13 and 14. However, this pattern was not observed above 40 deg for $AR = 1.0$, as shown in Fig. 14(c). The line pattern disappears regardless of the aspect ratio when the flow totally separates from the wing surface. This leads to the negligible differences in C_L and C_D due to the aspect ratio at large angles, as shown previously. Figure 14 also shows the visualized results for $AR = 0.5$ (stall hysteresis was not observed in this case). Figures 14(d), 14(e) and 14(f) show that the flow pattern does not change due to variation in the angle of attack. Moreover, the observed oil flows are quite similar to those for $AR = 1.0$ shown in Figs. 14(a) and 14(b). Thus, there is no noticeable difference in the flow structure between the results with and without stall hysteresis.

It is known that aerodynamic hysteresis is relatively common for thick airfoils at low Reynolds numbers.[1–3] Marchman et al.[21] stated that stall hysteresis tends to disappear as the aspect ratio decreases toward unity. The hypothesis is found to contradict the experimental data in the present study. Here, the aspect ratios of their models were 4 and 2; the cross-sectional shapes of their wings are NACA 0012, 0015, and 0021 airfoils. As is well known, the aerodynamic hysteresis of thick airfoils is related to the behavior of laminar separation bubbles: aerodynamic hysteresis occurs due to a delay in the reformation of the separation bubble.[2,12] However, the flow structures of low-aspect-ratio wings at large angles completely differ from those dominated by the separation bubble, as shown in Figs. 13 and 14. Hence, it is thought that the difference in the flow structure causes the variation in the stall characteristics. The change in the flow structure occurs when the aspect ratio is sufficiently low.

4. Conclusions

The effect of the aspect ratio on the aerodynamic characteristics of low-aspect-ratio wings was investigated. The Reynolds number considered was 5.2×10^4. The aerodynamic coefficients measured were discussed using the analytical and visualization results. The following results were obtained in the present study.

The lift coefficient is sensitive to the aspect ratio, although the difference in the drag coefficient is relatively small. Moreover, it is found that a slight variation in aspect ratio leads to a significant change in aerodynamic characteristics when the aspect ratio is between 1.3 and 1.0. The lift-to-drag ratio also shows an aspect ratio dependency at low angles. The difference in the lift-to-drag ratio is mainly caused by the potential lift component. However, the aspect ratio dependency becomes negligibly small when the angle of attack is large. The stall characteristics of low-aspect-ratio wings are significantly sensitive to the aspect ratio when the aspect ratio is between 1.5 and 0.5. The stall angle increases considerably as the aspect ratio decreases toward 1.0. Increasing the stall angle is accompanied by a large change in the flow structure on the wing surface. Furthermore, it is found that hysteresis during a stall occurs when the aspect ratio is within a narrow range. The loop of the stall hysteresis enlarges at an aspect ratio of around 1.0. The flow structure for low-aspect-ratio wings is completely different from that for high-aspect-ratio wings when the angle of attack is large. This causes variations in the stall characteristics and aerodynamic hysteresis of low-aspect-ratio wings.

References

1) Mueller, T. J.: Low Reynolds Number Vehicles, AGARDograph 288, 1985.
2) Mueller, T. J.: The Influence of Laminar Separation and Transition on Low Reynolds Number Airfoil Hysteresis, *J. Aircraft*, **22** (1985), pp. 763–770.
3) Selig, M. S., Guglielmo, J. J., Broeren, A. P., and Giguère, P.: Experiments on Airfoils at Low Reynolds Numbers, AIAA Paper 1996-0062, 1996.
4) Mueller, T. J., Kellogg, J. C., Ifju, P. G., and Shkarayev, S. V.: *Introduction to the Design of Fixed-Wing Micro Air Vehicles Including Three Case Studies*, AIAA Education Series, Reston, 2006, pp. 1–107.
5) Shyy, W., Lian, Y., Tang, J., Viieru, D., and Liu, H.: *Aerodynamics of Low Reynolds Number Flyers*, Cambridge University Press, New York, 2008, pp. 1–77.
6) Okamoto, M. and Azuma, A.: Aerodynamic Characteristics at Low Reynolds Numbers for Wings of Various Planforms, *AIAA J.*, **49** (2011), pp. 1135–1150.
7) Mizoguchi, M. and Itoh, H.: Effect of Aspect Ratio on Aerodynamic Characteristics at Low Reynolds Numbers, *AIAA J.*, **51** (2013), pp. 1631–1639.
8) Torres, G. E. and Mueller, T. J.: Low-Aspect-Ratio Wing Aerodynamics at Low Reynolds Numbers, *AIAA J.*, **42** (2004), pp. 865–873.
9) Mizoguchi, M. and Yamaguchi, Y.: Aerodynamic Characteristics of Rectangular Flat Plate Wings in Low Reynolds Number Flows, *J. Jpn. Soc. Aeronaut. Space Sci.*, **60** (2012), pp. 121–127 (in Japanese).
10) Shields, M. and Mohseni, K.: Effects of Sideslip on the Aerodynamics of Low-Aspect-Ratio Low-Reynolds-Number Wings, *AIAA J.*, **50** (2012), pp. 85–99.
11) Schmitz, F. W.: Aerodynamics of the Model Airplane. Part 1. Airfoil Measurements, RSIC-721, 1967.
12) Marchman, J. F. and Abtahi, A. A.: Aerodynamics of an Aspect Ratio 8 Wing at Low Reynolds Numbers, *J. Aircraft*, **22** (1985), pp. 628–634.
13) Marchman, J. F., Sumantran, V., and Schaefer, C. G.: Acoustic and Turbulence Influences on Stall Hysteresis, *AIAA J.*, **25** (1987), pp. 50–51.
14) Marchman, J. F.: Aerodynamic Testing at Low Reynolds Numbers, *J. Aircraft*, **24** (1987), pp. 107–114.
15) Hoffmann, J. A.: Effects of Freestream Turbulence on the Performance Characteristics of an Airfoil, *AIAA J.*, **29** (1991), pp. 1353–1354.
16) Grundy, T. M., Keefe, G. P., and Lowson, M. V.: Effects of Acoustic Disturbances on Low Reynolds Number Aerofoil Flows, *Prog. Astro. Aero.*, **195** (2001), pp. 91–113.
17) Winter, H.: Flow Phenomena on Plates and Airfoils of Short Span, NACA TM-798, 1936.
18) Ananda, G. K., Sukumar, P. P., and Selig, M. S.: Low-to-Moderate Aspect Ratio Wings Tested at Low Reynolds Numbers, AIAA Paper 2012-3026, 2012.
19) Kajikawa, Y., Mizoguchi, M., and Itoh, H.: On the Stall Hysteresis of Low-Aspect-Ratio Wings at Low Reynolds Numbers, JSASS-2013-5088, 2013 (in Japanese).
20) Marchman, J. F., Abtahi, A. A., Sumantran, V., and Sun, Z.: Effects of Aspect Ratio on Stall Hysteresis for the Wortmann Airfoil, AIAA Paper 1985-1770, 1985.
21) Marchman, J. F., Gunther, C. L., and Gundlach, J. F.: Semi-Span Testing at Low Reynolds Number, AIAA Paper 1998-0608, 1998.
22) Shindo, S.: Simplified Tunnel Correction Method, *J. Aircraft*, **32**

(1995), pp. 210–213.
23) Coleman, G. W. and Steele, W. G.: Engineering Application of Experimental Uncertainty Analysis, *AIAA J.*, **33** (1995), pp. 1888–1896.
24) Schlichting, H. and Truckenbrodt, E.: *Aerodynamics of the Airplane*, McGraw-Hill, New York, 1979, pp. 170–172.
25) Lamar, J. E.: Extension of Leading-Edge-Suction Analogy to Wings with Separated Flow around the Side Edges at Subsonic Speeds, NASA TR R-428, 1974.
26) Mizoguchi, M., Kajikawa, Y., and Itoh, H.: Static Stall Hysteresis of Low-Aspect-Ratio Wings, AIAA Paper 2014-2014, 2014.
27) Winkelmann, A. E. and Barlow, J. B.: Flowfield Model for a Rectangular Planform Wing beyond Stall, *AIAA J.*, **18** (1980), pp. 1006–1008.
28) Yon, S. A. and Katz, J.: Study of the Unsteady Flow Features on a Stalled Wing, *AIAA J.*, **36** (1998), pp. 305–312.

J. Cho
Associate Editor